Measurements of Hyperpolarized He-3 T2* and ADC in the Lungs Using Multi-echo VIPR

J. Holmes[1], R. O'Halloran[1], E. Brodsky[2,3], W. Block[2,3], and S. Fain[1,3]

[1]Medical Physics, University of Wisconsin-Madison, Madison, WI, United States, [2]Biomedical Engineering, University of Wisconsin-Madison, Madison, WI, United States, [3]Radiology, University of Wisconsin-Madison, Madison, WI, United States

Introduction

Lung tissue microstructure has been measured using diffusion weighted MRI and shown to be an early indicator of disease [1]. T_2* imaging using a radial outward PR (PRojection acquisition) trajectory with different echo times acquired over multiple breath-holds has been demonstrated to correlate with O_2 concentration and tissue microstructure [2]. The use of multi-echo PR has been demonstrated for high resolution, rapid imaging of HP He-3 spin-density in the lungs [3]. These multi-echo PR trajectories are appealing for T_2* mapping [4] as well as for providing isotropic resolution for diffusion weighted imaging to probe tissue microstructure.

Methods

A multi-echo PR trajectory acquiring 8 half-echos [5] was used to measure H-1 T_2* values in a Gd-DTPA T_2* phantom and He-3 values in a volunteer. He-3 acquisition parameters included 20 s acquisition time, BW = +/- 125 kHz, FOV = 42 cm, 128 acquisition matrix, and 1 L inhaled dose of 5.6 mM He-3 mixed with N_2 was delivered. A modulated flip angle was implemented to uniformly utilize the finite magnetization over each excitation [6]. Sampling during gradient ramping was performed to reduce the echo time and improve data collection efficiency. To combine data from ramp samples and multiple echos effectively, we characterize the gradients and use this information to properly regrid the data [7]. Data was reconstructed to provide images at separate individual echo times (k_r = 0) of 1.016 ms, 1.736 ms, and 2.456 ms where both positive and negative k_z hemispheres have been sampled. A mono-exponential model was linearized and used to fit the logarithm of the signal decay. For comparison, a standard 2D Cartesian multi-echo FGRE scan was also used to measure the T_2* values in the Gd-DTPA phantom. Scan parameters for the 2D Cartesian scan were TR = 150 ms, FOV = 25 cm x 25 cm, Slice thickness = 2 cm, and 16 echos acquired from 3.1 to 87 ms. Diffusion weighted imaging was performed using a 4 half-echo acquisition to reduce blurring during the data readout due to T_2*. Diffusion sensitizing bi-polar gradients along the patient S/I direction were placed before the data acquisition window, extending the TR/TE to 6.3 ms / 3.3 ms. Data was collected over a 40 s breath-hold with each projection acquired with and without diffusion weighting. Further, 10 unique projection angle sets were acquired to distribute uncorrected signal modulations from T_1 decay of the gas and RF depletion.

Table 1. Summary of T_2* results from Gd-DTPA phantom using 2D Cartesian multi-echo FGRE and the multi-echo 3D PR acquisitions.

ROI	Gd-DTPA (mM)	T_2* 2D multi-echo FGRE (ms)	R^2	T_2* 3D PR (ms)	R^2
1	0	61.66	0.99	49.46	0.83
2	2	38.16	0.99	39.18	0.83
3	4	16.94	0.99	28.85	0.99
4	8	15.83	0.99	20.30	0.94
5	16	11.46	0.99	18.41	0.94
6	32	6.10	0.98	7.18	0.99

Table 4. Summary of T_2* results for HP He-3 in a volunteer for selected ROIs. Two separate ROIs were taken in the parenchyma.

ROI	T_2* 3D PR (ms)	R^2
Trachea	17.6	0.99
Parenchyma 1	14.3	0.51
Parenchyma 2	20.7	0.99
Near blood vessel	8.2	0.99

Results

H-1 T_2* values measured in the phantom studies using the multi-echo PR acquisition are in reasonable agreement with those measured using the 2D multi-echo FGRE T_2* acquisition (Table 1) although the goodness of fit (R^2) decreases with longer T_2* time (>16 ms) as the decay curve has been insufficiently sampled. HP He-3 T_2* analysis was performed in a volunteer (Fig. 1) and T_2* values for specific ROIs are reported in Table 1. The coronal T_2* map depicts shortened T_2* near the aorta and diaphragm (Fig 1b). Further, the axial T_2* map shows evidence of gravity dependence with shorter times near the apex with longer values near the base. Results from diffusion weighted imaging are reconstructed to a 64^3 matrix in order to provide sufficient SNR for calculating the ADC (Figure 2). ADC values measured in the trachea were 1.3 cm^2/s and in the parenchymal space were 0.3 cm^2/s similar to those found with more conventional 2D multi-slice ADC acquisitions.

Figure 1. a) 8 half-echo HP He-3 spin-density image using data from all echos, b) coronal and c) axial HP He-3 $1/T_2$* image of a volunteer. Note shortened T_2* near the aorta and diaphragm due to susceptibility and gravity dependence evident in the axial view.

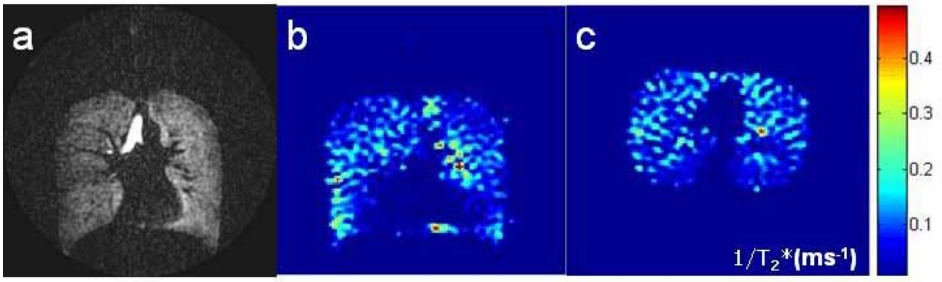

Conclusions and Discussion

The use of an 8 half-echo PR trajectory is shown for T_2* mapping in the lungs in a single breath-hold. In the current implementation, datasets from 3 echo times are used to estimate the T_2*. Also the use of multi-echo PR for isotropic ADC imaging is demonstrated. The imaging gradients of these multi-echo acquisitions use high slew rates and large amplitudes to allow rapid coverage of k-space resulting in diffusion weighting of the data sampled during later echos in a single TR, particularly the 8 half-echo acquisition. Diffusion weighting due to the gradients was not directly accounted for in the T_2* analysis however future work will include modification of the trajectory to acquire additional echos to allow multi-exponential fits to the signal decay. Further, implementation of a diffusion weighted multi-echo PR acquisition with true 3D weighting is underway.

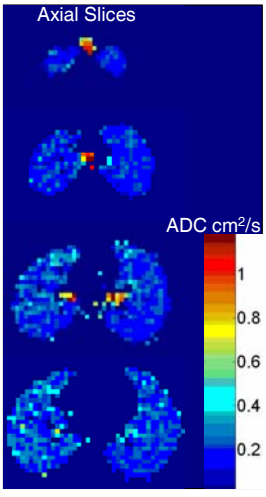

Figure 2. Subset of axial ADC images acquired at isotropic resolution using the 4 half-echo 3D PR trajectory. Diffusion values in the trachea and parenchyma are consistent with those found in 2D multi-slice acquisitions (the standard for HP He-3 diffusion imaging).

References

[1] Fain et al. Radiology 2006;235:875-883.
[2] Chen et al. MRM 1999 ;42 :729-737.
[3] Holmes et al. ISMRM 14:867(2006)
[4] Song et al. MRM 2000;44 :825-832
[5] Brodsky et al. ISMRM 11:322 (2005)
[6] Miller et al. MAGMA 2004 ;16 :218-226
[7] Duyn et al. JMR 1998;132:150-153